Without interstate mixing the conjugate does not function as a phototropic assembly, and absorbed photons are converted into heat within about 50 ps. Interstate mixing extends the overall timescale for charge recombination to about 40 µs, but the phototropic process itself continues for milliseconds. This is because diffusional charge recombination occurs between separated π radical cations, and is followed by slower reinsertion of the dication into the receptor (see Figure 1). In contrast to the case with $MV \cdot 2PF_6$, where the acceptor is nonfluorescent and separation of the RIP is minimal, formation of free $DAP \cdot 2PF_6$ as a transitory species can be followed by fluorescence spectroscopy using two-color (or delayed pulse) excitation. Background fluorescence, being set by the amount of free $DAP \cdot 2PF_6$, can be suppressed with excess CE10, while the rate of reinsertion of $DAP \cdot 2PF_6$ into the cavity is solvent-dependent. Similar behavior is found for $ADIQ \cdot 2PF_6$, but the level of background fluorescence is too high for practical application. With complex **1**, however, laser-induced fluorescence selectively tracks the evolution and disappearance of free diazapyrenium dications.

Experimental Section

$DAP \cdot 2PF_6$ [11] and CE10 [17] were prepared by literature methods. $ADIQ \cdot 2PF_6$ was available from earlier work [11]. All compounds gave satisfactory analytical data that were consistent with their assigned structures. Fast kinetic measurements were made with nanosecond and sub-picosecond laser flash photolysis equipment, built for this purpose, similar to that described previously [11]. The excitation wavelength was 440 nm. Decay kinetics were obtained by collecting transient differential absorption spectral profiles at about 50 delay times. Binding constants were determined by fluorescence spectroscopy with about 50 different concentrations of crown ether being added to a solution of fluorophore in acetonitrile.

X-ray structure analysis of **1**: $C_{48}H_{54}F_{12}N_3O_{10}P_2$, $M_r = 1122.88$, yellow prisms, $0.15 \times 0.20 \times 0.45$ mm, measured at 293(2) K; triclinic, $P\bar{1}$, $a = 11.284(2)$, $b = 11.211(2)$, $c = 12.043(2)$ Å, $\alpha = 99.95(3)$, $\beta = 106.28(3)$, $\gamma = 107.15(3)°$, $V = 1342(4)$ Å^3, $\rho_{calcd} = 1.389$ mg m^{-3}, Enraf-Nonius CAD-4 diffractometer, $Mo_{K\alpha}$ radiation ($\lambda = 0.71069$ Å), $\mu = 0.179$ mm^{-1}, $\omega/2\theta$ scan, $2\theta \leq 60°$; of 7524 reflections measured, 6509 were independent; ψ-scan absorption correction, $T_{min} = 0.94$, $T_{max} = 1.00$. The structure was solved with direct methods (SHELXS-86), and refined on F^2 (SHELXL-93; non-hydrogen atoms, except disordered F atoms, were refined anisotropically, and H atoms at calculated positions in riding mode). $R_1 = 0.0959$ for 6494 reflections ($F_0 \geq 4\sigma(F)$), $wR_2 = 0.2949$ for all data, GOF = 1.0086, 330 parameters, $\Delta\rho_{max} = 1.042$ e Å^{-3} in the vicinity of a severely disordered solvent molecule. Crystallographic data (excluding structure factors) for the structures reported in this paper have been deposited with the Cambridge Crystallographic Data Centre as supplementary publication no. CCDC-100343. Copies of the data can be obtained free of charge on application to The Director, CCDC, 12 Union Road, Cambridge CB21EZ, UK (fax: int. code +(1223)336-033; e-mail: deposit@chemcrys.cam.ac.uk).

Received: May 28, 1997 [Z10407IE]
German version: *Angew. Chem.* **1997**, *109*, 2451–2454

Keywords: charge transfer · crown compounds · fluorescence spectroscopy · photochemistry · polycycles

---

[1] a) A. C. Benniston, A. Harriman, *Angew. Chem.* **1993**, *105*, 1553–1555; *Angew. Chem. Int. Ed. Engl.* **1993**, *32*, 1459–1461; b) A. C. Benniston, *Chem. Soc. Rev.* **1996**, *25*, 427–435.
[2] M. Seiler, H. Dürr, *Liebigs Ann.* **1995**, 407–409.
[3] R. Ballardini, V. Balzani, M. T. Gandolfi, L. Prodi, M. Venturi, D. Philp, H. G. Ricketts, J. F. Stoddart, *Angew. Chem.* **1993**, *105*, 1362–1364; *Angew. Chem. Int. Ed. Engl.* **1993**, *32*, 1301–1304.
[4] A. C. Benniston, A. Harriman, V. M. Lynch, *J. Am. Chem. Soc.* **1995**, *117*, 5279–5291.
[5] a) A. C. Benniston, A. Harriman, D. Philp, J. F. Stoddart, *J. Am. Chem. Soc.* **1993**, *115*, 5298–5299; b) A. C. Benniston, A. Harriman, *ibid.* **1994**, *116*, 11531–11537.
[6] J. N. Murrell, *J. Am. Chem. Soc.* **1969**, *81*, 5037–5043.
[7] M. Bixon, J. Jortner, J. W. Verhoeven, *J. Am. Chem. Soc.* **1994**, *116*, 7349–7355.
[8] a) I. R. Gould, J. E. Moser, D. Ege, S. Farid, *J. Am. Chem. Soc.* **1988**, *110*, 1991–1993; b) A. M. Brun, A. Harriman, S. M. Hubig, *J. Phys. Chem.* **1992**, *96*, 254–257.
[9] A. C. Benniston, V. Grosshenny, A. Harriman, R. Ziessel, *Angew. Chem.* **1994**, *106*, 1956–1957; *Angew. Chem. Int. Ed. Engl.* **1994**, *33*, 1884–1885.
[10] A. C. Benniston, A. Harriman in *NATO ARW Physical Supramolecular Chemistry* (Eds.: A. E. Kaifer, L. Echegoyen), in press.
[11] A. M. Brun, A. Harriman, *J. Am. Chem. Soc.* **1991**, *113*, 8153–8159.
[12] P. R. Ashton, S. J. Langford, N. Spencer, J. F. Stoddart, A. J. P. White, D. J. Williams, *Chem. Commun.* **1996**, 1387–1388.
[13] B. L. Allwood, N. Spencer, H. Shahriari-Zavareh, J. F. Stoddart, D. J. Williams, *J. Chem. Soc. Chem. Commun.* **1987**, 1064–1066.
[14] S. Khazaeil, A. I. Popov, J. L. Dye, *J. Phys. Chem.* **1983**, *87*, 1832–1833.
[15] Complexation of higher order causes a slight curvature of the plateau region at high mole fractions of CE10. Such behavior is not seen in the mass-spectral studies. Formation of a 1:1 complex for $ADIQ \cdot 2PF_6$ in [D$_6$]acetone causes upfield shifts of −0.15, −0.13, and −0.022 ppm for the α, β, δ protons, respectively. Formation of a 1:2 complex causes further upfield shifts of −0.083 (α), −0.070 (β), and −0.012 ppm (δ). Both complexes are observed by FAB mass spectrometry in acetonitrile.
[16] These energy gaps, which are crudely estimated from absorption maxima of the lowest-energy π–π* transition localized on the acceptor and the CT transition are 1.6, 0.15, and −0.3 eV for $MV \cdot 2PF_6$, $DAP \cdot 2PF_6$, and $ADIQ \cdot 2PF_6$, respectively. For the latter, the CT band lies at higher energy than the lowest-energy π–π* transition.
[17] P. L. Anelli, P. R. Ashton, R. Ballardini, V. Balzani, M. Delgado, M. T. Gandolfi, T. T. Goodnow, A. E. Kaifer, D. Philp, M. Pietraszkiewicz, L. Prodi, M. V. Reddington, A. M. Z. Slawin, N. Spencer, J. F. Stoddart, C. Vicent, D. J. Williams, *J. Am. Chem. Soc.* **1992**, *114*, 193–218.

Novel Zwitterionic Diallylzirconium Complexes: Synthesis, Structure, Polymerization Activity, and Deactivation Pathways[**]

Gerardo Jiménez Pindado, Mark Thornton-Pett,
Marco Bouwkamp, Auke Meetsma, Bart Hessen,[*]
and Manfred Bochmann[*]

Group 4 metallocene complexes are becoming increasingly important as "single-site" catalysts for the polymerization of α-olefins,[1] and the number of industrial processes based on Cp complexes is growing rapidly.[2] The catalytically active species are electron-deficient complexes of the type $[Cp_2MR]^+$ (M = Ti, Zr, Hf), which are usually generated in situ by reacting a neutral metal alkyl complex with cation-generating activators such as methylaluminoxane (MAO) or, in aluminum-free systems, $M^+[B(C_6F_5)_4]^-$ ($M = HNMe_2Ph$, CPh_3), to give ion pairs $[Cp_2MR]^+X^-$ [$X = Me\text{-}MAO$, $B(C_6F_5)_4$].[1] Zwitterionic complexes such as $[Cp^*_2Zr(m\text{-}C_6H_3Et)B(C_6H_4Et)_3]$, $[Cp_2ZrMe(\mu\text{-}Me)B(C_6F_5)_3]$, $[Cp^*TiMe_2(\mu\text{-}Me)B(C_6F_5)_3]$ (Cp* = tetramethylcyclopentadienyl), $[Zr(CH_2Ph)_3(\eta\text{-}Ph)BPh_3]$, and $[Zr(CH_2Ph)_3(\eta^6\text{-}PhCH_2)B(C_6F_5)_3]$ have proved to be useful catalyst precursors;[3–7] here the active species is generated by dissociation into ion pairs. More recently Erker et al. prepared zwitterionic allylic complexes $[Cp_2M(\eta^3\text{-}C_3H_4CH_2)B(C_6F_5)_3]$ by treating zirconocene and hafnocene butadiene complexes with $B(C_6F_5)_3$. These compounds are less electron-deficient than the alkyl complexes mentioned above and achieve an electron count of 18 through a weak Zr–F coordination.[8]

Structural and catalytic studies have so far mainly concentrated on the chemistry of highly reactive 14-electron alkyl complexes $[Cp_2MMe]^+$ (M = Ti, Zr, Hf). The isoelectronic cationic

---

[*] Prof. Dr. M. Bochmann, Dr. G. Jiménez Pindado, Dr. M. Thornton-Pett
School of Chemistry, University of Leeds
Leeds LS2 9JT (UK)
Fax: Int. code +(113) 233 6401
e-mail M.Bochmann@chem.leeds.ac.uk

Dr. B. Hessen, M. Bouwkamp, Dr. A. Meetsma
Department of Chemistry, University of Groningen
Nijenborgh 4, NL-9747 AG Groningen (The Netherlands)
e-mail hessen@chem.rug.nl

[**] This work was supported by the Engineering and Physical Sciences Research Council. G. J. P. thanks the Science and Education Ministry of Spain for a research fellowship.

diallyl complexes of the type $[CpM(\eta^3\text{-allyl})_2]^+$ should exhibit a similarly promising reactivity. We describe here the synthesis, catalytic activity, and structural characterization of the first zwitterionic diallylzirconium complexes. The ability of these species to undergo unusually facile C–H activation illustrates the remarkable difference in reactivity between mono-Cp $[CpM(allyl)_2]^+$ ions and the more familiar metallocene analogues $[Cp_2MR]^+$ (R = alkyl, allyl).

Treatment of a solution of $[Cp''Zr(\eta^3\text{-}C_3H_5)\{\eta^4\text{-}CH_2C(Me)C(Me)CH_2\}]$ (**1a**) [$Cp'' = 1,3\text{-}(SiMe_3)_2C_5H_3$] in toluene with $B(C_6F_5)_3$ at −78 °C leads to a color change from red to orange. Monitoring this reaction by NMR spectroscopy in CD_2Cl_2 between −70 and 20 °C reveals the formation of a single chiral complex; seven ^{1}H NMR resonances for allylic ligands (five from the $\eta^3\text{-}C_3H_5$ ligand, two from the η^3-dienyl unit) appear together with two broadened doublets for the $\text{-}CH_2\text{-}B$ moiety at $\delta = -0.33$ and -1.78 (Table 1). These data are consistent with an attack by $B(C_6F_5)_3$ exclusively on one of the terminal carbon atoms of the diene ligand to give the zwitterionic diallyl complex **2a** [Eq. (a)]. The unusually high-field shifted ^{1}H NMR resonances for the $CH_2{-}B$ moiety suggest possible $C{-}H\cdots Zr$ bonding.

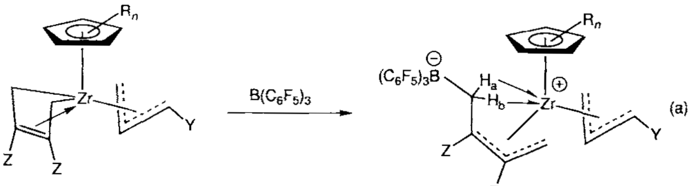

1a, $R_n = 1,3\text{-}(SiMe_3)_2$; Y = H, Z = Me
1b, $R_n = 1,3\text{-}(SiMe_3)_2$; Y = Me, Z = H
1c, $R_n = Me_5$; Y = Me, Z = H

2a - c

The ^{11}B NMR singlet of **2a** at $\delta = -12.0$ confirms the formation of a triarylborate. The ^{19}F NMR spectrum shows six resonances for the *ortho*-F atoms of three inequivalent C_6F_5 groups, whose rotation about the $B{-}C_6$ and $B{-}CH_2$ bonds is evidently highly hindered. All six *o*-F signals have chemical shifts between $\delta = -129$ and -135 and remain unchanged on cooling to −85 °C; a high-field shift of one of the *o*-F signals, which might indicate a metal–fluorine coordination,[9] is not observed.

Compound **2a** is isolated as air-sensitive orange crystals (83% yield) that are thermally stable at room temperature. Cooling solutions of **2a** in toluene to −16 °C afforded orange-yellow crystals of **2a**·toluene suitable for X-ray diffraction.[10] The sterically demanding ligands of the zwitterionic molecule (Figure 1) prevent any close intra- or intermolecular $M\cdots F$ interactions. The Zr–C distances in the $[Cp'Zr(allyl)_2]^+$ core correspond closely to the values of the neutral allyl precursor. The cationic 14-electron fragment is stabilized by two agostic interactions with the $B{-}CH_2$ group [$Zr\cdots H$ 2.29(5) and 2.30(5) Å].[11]

Compound **2a** crystallizes with one molecule of toluene, which in the crystal is associated with one of pentafluorophenyl rings; the distances between the plane of the six-membered ring of the toluene molecule and the best least-squares plane through the C_6F_5 group are relatively short (3.17–3.45 Å). This solvent binding is reminiscent of the well known 1:1 stacking phases formed between benzene and hexafluorobenzene.[12]

Mixtures of **1a** activated with one equivalent $B(C_6F_5)_3$ in toluene catalyze the polymerization of ethene under mild conditions (Table 2). While the M_w values are within the expected range, the broadening of the polydispersities with rising poly-

Table 1. Selected spectroscopic data.

2a: ^{1}H NMR (300 MHz, CD_2Cl_2, −40 °C; C atom numbering as in Figure 1): $\delta = -1.78$, −0.33 (br s, 1 H each; H_2CB), 0.19, 0.36 (s, 9 H each; SiMe), 1.41, 2.52 (d, $J = 8.3$ Hz, 1 H each; CCH_2), 1.68, 1.76 (s, 3 H each, diene-Me); 1.96 (m, 2 H), 2.66 (br. d, 1 H), 3.19 (d, $J = 15.3$ Hz 1 H; 14 or 16-CH_2), 5.96 (m, 1 H, 15-CH), 6.51, 6.96 (m, 1 H, 4,5-C_5H_3), 6.44 (m, 1 H, 2-C_5H_3); ^{13}C NMR (75.4 MHz, CD_2Cl_2, −40 °C): $\delta = -0.55$, −0.23 (q, $J = 119.1$, 119.6 Hz; SiMe), 16.93, 23.77 (q, $J = 129.5$, 127.8 Hz, diene-Me), 31.09 (vbr. t, CH_2B), 59.64 (t, $J = 150.1$ Hz, CCH_2), 67.12, 71.03 (t, $J = 155.9$, 158.6 Hz; CH_2 of C_3H_5), 112.91 (m, 8-C), 117.53 (d, $J = 170.5$ Hz; 2-C_5H_3), 124.0, 131.45 (d, $J = 169.8$, 172.0 Hz; 4,5-C_5H_3), 125.28, 129.26 (m, 1,3-C_5H_3), 138.06 (m, 7-C), 140.77 (d, $J = 153.2$ Hz, 11-CH); ^{11}B NMR (96.2 MHz, CD_6Cl_2, −40 °C): $\delta = -11.99$; ^{19}F NMR (CD_2Cl_2, −50 °C): $\delta = -129.6$, −132.2, −130.0, −132.6, −134.0, −134.7 (d, $^3J(F,F) = 19.6$ Hz, 1 F each; *o*-F), −159.9, −160.1, −160.6 (t, $^3J(F,F) = 19.7$ Hz, 1 F each; *p*-F); −164.2, −165.1, −165.6, −167.0 (m, 2 F, 1 F, 2 F, 1 F; *m*-F)

2b: ^{1}H NMR ([D$_8$]toluene, 300 MHz, −30 °C): $\delta = -1.68$ (s, br, 1 H; BCH_2), −1.58 (d, $J = 14.4$ Hz, 1 H; BCH_2), −0.22, 0.09 (s, 9 H each; SiMe), 0.92 (d, $J = 5.61$ Hz, 3 H; Me), 2.21, 1.98 (m, 1 H; diene-CH_2), 1.65, 2.00 (dd, $J = 13.4$, 3 Hz, 1 H; CH_2 of C_4H_7), 1.71 (m, 1 H; C*H*Me of C_4H_7), 4.58 (dd, $J = 14.0$, 9.9 Hz, 1 H; diene-CH), 5.01 (m, 1 H; CH of C_4H_7), 5.17 (m, 1 H; diene-CH), 5.87, 5.93, 6.63 (m, each 1 H, C_5H_3); ^{13}C NMR ([D$_8$]toluene, −50 °C): $\delta = -0.91$, −0.71 (SiMe), 18.49 (Me), 28.0 (br., BCH_2), 57.58 (diene-CH_2), 61.18 (CH_2 of C_4H_7), 83.45 (diene-*C*HMe), 106.45 (diene-CH), 118.56, 124.43, 125.61 (2,4,5-C_5H_3), 126.35 (br., 1,3-C_5H_3), 133.09 (diene-CH), 137.37 (CH of C_4H_7), 137.23 ($J(C,F) = 242.25$ Hz, *m*-C, C_6F_5), 139.42 ($J(C,F) = 235.0$ Hz, *p*-C, C_6F_5), 148.23 ($J(C,F) = 238.47$ Hz, *o*-C, C_6F_5); ^{11}B{^{1}H} NMR ([D$_8$]toluene, −60 °C): $\delta = -12.58$; ^{19}F NMR ([D$_8$]toluene, −60 °C): $\delta = -131.2$, −132.9, −135.1 (br. s, 1 F, 4 F, and 1 F; *o*-F); −158.9 (vbr. s, 3 F; *p*-F); −164.3 (br. s, 6 F, *m*-F)

3a: ^{1}H NMR (300 MHz, −20 °C): $\delta = -1.87$ (br. s, 1 H; BCH_2); 0.12, 0.23 (s, 9 H each; SiMe); 1.29 (d, $J = 5.4$ Hz; 1 H, $=CH_2$ of diene), 1.49 (br. s, 1 H, BCH_2), 1.67 (s, 9 H; CMe_3), 1.80, 2.05 (s, 3 H each; diene-Me), 2.06 (d, $J = 16.0$ Hz 1 H; CH_2 of C_3H_5), 2.18 (m, 1 H, $J = 16.0$ Hz; CH_2 of C_3H_5), 2.28 (d, $J = 5.4$ Hz, 1 H; $=CH_2$ of diene), 3.66, 3.97 (m, 1 H each; CH_2 of C_3H_5), 5.00, 5.01, 5.33 (m, 1 H each; C_5H_3), 5.15 (m, 1 H; CH of C_3H_5); ^{13}C NMR (CD_2Cl_2, −20 °C): $\delta = -0.27$, −0.03 (q, $J = 119.3$ Hz; SiMe), 21.83, 24.93 (q, $J = 125.0$, 126.3 Hz; diene-Me), 26.72 (br. s, BCH_2), 29.64 (q, $J = 129.5$ Hz; $C(CH_3)_3$), 47.1 (t, $J = 151.0$ Hz; diene-CH_2), 60.09 (s, *C*Me$_3$), 61.05, 68.25 (t, $J = 158.8$, 161.0 Hz; CH_2 of C_3H_5), 109.1 (d, $J = 170.0$ Hz; 2-C_5H_3), 117.71 (d, $J = 172.8$ Hz; 4,5-C_5H_3), 118.03, 118.81 (s, =*C*Me), 120.20 (m, 1,3-C_5H_3), 120.89 (t, $J = 150.1$ Hz; CH of C_3H_5), 124.6 (*ipso*-C, BC_6F_5), 136.54 ($J(C,F) = 255.8$ Hz; *m*-C, C_6F_5), 138.24 ($J(C,F) = 249.7$ Hz; *p*-C, C_6F_5), 147.97 ($J(C,F) = 247.5$ Hz; *o*-C, C_6F_5), 159.06 (s, CN); ^{11}B{^{1}H} NMR (CD_2Cl_2, −20 °C): $\delta = -14.02$; ^{19}F NMR (CD_2Cl_2, 10 °C): $\delta = -131.5$ (t, br, 6 F; *o*-F), −163.1 (t, $^3J(F,F) = 19.8$ Hz, 3 F; *p*-F); −167.1 (br. 6 F; *m*-F)

4b: ^{1}H NMR ([D$_8$]toluene, 300 MHz, 25 °C): $\delta = -0.14$, 0.05 (s, each 9 H; SiMe), 0.59, 2.19 (t, br, $J = 8.9$ Hz, each 1 H; CH_2), 2.21 (d, $J = 12.6$ Hz, 1 H; BCH), 5.99 (t, br, 1 H, C*H*=CB), 6.23 (q, $J = 9.2$ Hz, 1 H; $CH_2{=}CH$), 6.48 (t, $J = 2.2$ Hz, 1 H; 2-C_5H_3), 6.65, 7.59 (br. s, 1 H each; 4.5-C_5H_3); ^{13}C NMR (CD_2Cl_2, −20 °C): $\delta = -0.95$, −0.73 (q, $J = 119.5$ Hz; SiMe), 67.62 (t, $J = 150.0$ Hz; CH_2), 93.64 (d, $J = 136.56$ Hz; BCH), 120.54, 129.53 (d, $J = 170.55$, 160.74 Hz; 4,5-C_5H_3), 124.65 (d, $J = 167.53$ Hz; *C*H=CB), 127.22 (d, $J = 169.04$ Hz; 2-C_5H_3), 135.64 (d, $J = 166.02$ Hz; $H_2C{=}CH$), 127.40, 134.56 (m; 1,3-C_5H_3); ^{11}B{^{1}H} NMR ([D$_8$]toluene, 15 °C): $\delta = 43$ (br. s); ^{19}F NMR ([D$_8$]toluene, −40 °C): *o*-F: $\delta = -114.1$ (br. s; 2 F), −130.1 (d, $J(F,F) = 19.7$ Hz, 2 F), −130.6 (br. s; 1 F), −169.9 (br. s, 1 F), *p*-F: $\delta = -149.3$ (br. s; 1 F), −150.7 (t, 1 F, $J(F,F) = 21.1$ Hz), −153.6 (t, 1 F; $J(F,F) = 19.7$ Hz); *m*-F: $\delta = -156.2$, −156.5 (br. s, 1 F each, overlaps with the *m*-F signal of **4b'**), −161.2 (m, 4 F)

4b': ^{1}H NMR ([D$_8$]toluene, 300 MHz, 25 °C): $\delta = -0.15$, 0.03 (s, 9 H, SiMe), 1.44 (m, 1 H), 3.42 (dd, $J = 7.6$, 6.6 Hz, 1 H; CH_2), 5.10 (m, 1 H; $H_2C{=}CH$), 5.34 (d, $J = 12.0$ Hz; BCH), 5.82 (m, 1 H; C*H*=CB), 5.97, 7.01 (m, 1 H each; 4,5-C_5H_3), 7.71 (t, $J = 1.9$ Hz, 1 H, 2-C_5H_3); ^{13}C NMR (CD_2Cl_2, −20 °C): $\delta = -1.39$, −0.47 (q, $J = 119.6$ Hz; SiMe), 82.31 (t, $J = 152.82$ Hz; CH_2), 97.17 (d, $J = 136.2$ Hz, BCH), 123.96, 134.05 (m, 1,3-C_5H_3), 125.68 (*C*H=CB); 125.9, 128.13 (4,5-C_5H_3); 129.68 (d, $J = 165.0$ Hz; $H_2C{=}CH$), 135.11 (d, $J = 172.06$ Hz; 2-C_5H_3); ^{11}B{^{1}H} NMR ([D$_8$]toluene, 15 °C): $\delta = 43$ (br. s); ^{19}F NMR ([D$_8$]toluene, −40 °C): *o*-F: $\delta = -118.7$ (d, $J(F,F) = 25.4$ Hz, 2 F), −129.4 (br. s, 1 F), −131.4 (d, $J(F,F) = 16.9$ Hz, 2 F), −184.1 (br. s, 1 F); *p*-F: $\delta = -151.6$, −155.3 (t, 1 F each, $J(F,F) = 19.7$ Hz), −152.2 (t, 1 F, $J(F,F) = 21.1$ Hz); *m*-F: $\delta = -156$ (1 F, overlaps with the *m*-F signal of **4b**), −157.1 (br. s, 1 F), −160.5, −162.2 (m, 2 F each)

4c: ^{1}H NMR ([D$_8$]toluene, 500 MHz, −30 °C): $\delta = 1.53$ (s, 15 H; Cp*), 2.38 (m, 1 H; C*H*H), 2.63 (t, $J = 7.0$ Hz, 1 H; CH*H*), 4.68 (br. m, 1 H; C*H*=CB), 5.04 (m, 1 H; $CH_2{=}CH$), 5.85 (d, $J = 12.7$ Hz, 1 H; BCH); ^{13}C{^{1}H} NMR ([D$_8$]toluene, 125 MHz, −30 °C): $\delta = 10.96$ (Cp*-Me), 77.81 (CH_2), 95.94 (BCH), 124.08 (Cp* ring), 125.95 (*C*H=CB), 126.91 ($H_2C{=}CH$); ^{19}F NMR (C_6D_5Br, 282 MHz, −30 °C): *o*-F: $\delta = -120.3$ (1 F), −130.5 (br., 1 F), −130.55 (d, $J(F,F) = 15$ Hz; 2 F), −136.5 (br., 1 F), −180.0 (br., 1 F); *p*-F: $\delta = -153.5$ (t, $J(F,F) = 21$ Hz, 1 F), −154.2 (t, $J(F,F) = 21$ Hz, 1 F), −156.0 (t, $J(F,F) = 20$ Hz, 1 F); *m*-F: $\delta = -158.4$ (br, 1 F), −159.2 (m, 1 F), −160.2 (br, 1 F), −161.9 (m, 1 F), −163.7 (m, 2 F).

0570-0833/97/3621-2359 $ 17.50+.50/0

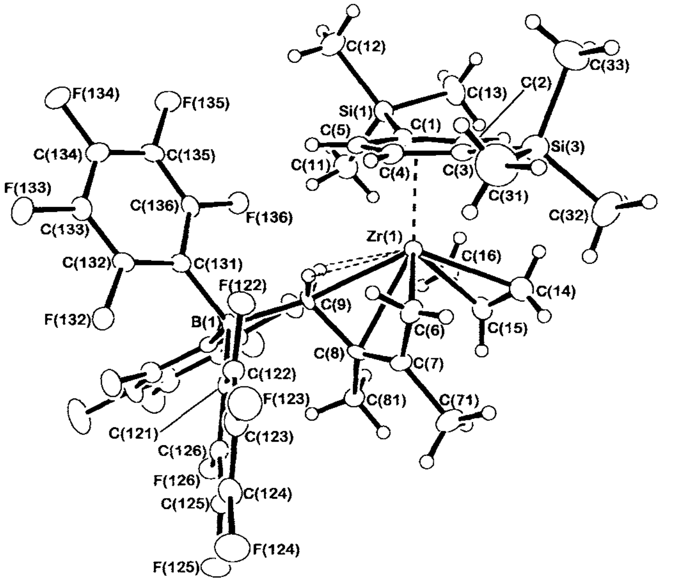

Figure 1. Structure of **2a** (ORTEX [22] diagram). Thermal ellipsoids are shown at the 40% probability level. Selected bond lengths [Å] and angles [°]: Zr(1)–C(6) 2.331(5), Zr(1)–C(7) 2.525(4), Zr(1)–C(8) 2.450(4), Zr(1)–C(9) 2.442(4), Zr(1)–C(14) 2.443(5), Zr(1)–C(15) 2.492(6), Zr(1)–C(16) 2.438(6), Zr(1)–C(1) 2.521(4), Zr(1)–C(2) 2.500(4), Zr(1)–C(3) 2.527(4), Zr(1)–C(4) 2.509(5), Zr(1)–C(5) 2.484(4), Zr(1)–H(9a) 2.30(5), Zr(1)–H(9b) 2.29(5), C(6)–C(7) 1.425(7), C(7)–C(8) 1.388(7), C(8)–C(9) 1.508(6), C(9)–B(1) 1.714(6), C(14)–C(15) 1.393(8), C(15)–C(16) 1.395(8); C(7)-C(6)-Zr(1) 80.6(3), C(8)-C(9)-B(1) 116.9(4), C(8)-C(9)-Zr(1) 72.3(2), B(1)-C(9)-Zr(1) 169.6(3).

Table 2. Ethene polymerizations with **1a**/$B(C_6F_5)_3$ [a].

Temperature [°C]	Time [min]	Polymer yield [g]	Productivity [b] × 10^{-3}	M_w	M_w/M_n
0	3.5	0.144	98.7	201	3.5
20	5	0.132	63.3	181	4.7
44	10	0.180	43.2	107	5.2
60	10	0.190	45.6	77.3	7.6

[a] Conditions: **1a** (25 μmol), $B(C_6F_5)_3$ (25 μmol), toluene (20 mL), ethene 1 bar. [b] In 10^3 g PE (mol Zr)$^{-1}$ h^{-1}.

merization temperature to values significiantly higher than those typically obtained for metallocenes may suggest the loss of active site uniformity. Such behavior may offer advantages where the desired polymer properties or processing parameters favor broader polydispersities.[13, 14]

Treatment of **2a** with excess *tert*-butylisocyanide at 0 °C leads to the immediate formation of the adduct **3a** as yellow microcrystals. Rather unexpectedly, warming the reaction mixture did not lead to an isocyanide insertion product but to the quantitative regeneration of **1a**, together with tBuNC·$B(C_6F_5)_3$ ($\tilde{\nu}_{C\equiv N}$ = 2300 cm^{-1}), which, to our knowledge, is the first example of a fully reversible formation of a $[RB(C_6F_5)_3]^-$ borate unit. By contrast, di-Cp complexes such as $[Cp_2Zr\{C_3H_4CH_2-B(C_6F_5)_3\}]$ readily give the expected isocyanide insertion products.[8b]

The reaction of $B(C_6F_5)_3$ with the butadiene complexes **1b** and **1c** gives the corresponding zwitterionic complexes **2b** and **2c**, respectively. The spectroscopic data of these compounds are very similar to those of **2a**. Both catalyze the polymerization of ethene but are thermally less stable than the sterically more hindered **2a** and decompose by an unexpected C–H activation pathway, in which 2-butene is eliminated and a C_6F_5 group migrates from boron to zirconium to give **4** [Eq. (b)]. In the case

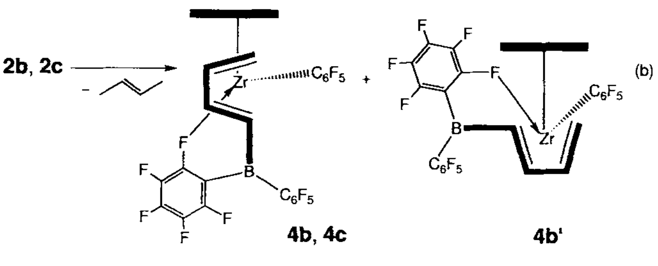

of **2b**, this reaction sequence is very facile even at −60 °C.[15] The transformation of the four-coordinate borate in **2b** into a three-coordinate boryl in **4b** is reflected in the change in the ^{11}B NMR signal from about $\delta = -12$ to $\delta = +43$. Compound **4b** is accompanied by a second, fluxional isomer **4b'**. The C_5Me_5 complex **2c** is more stable and rearranges to **4c** with $\tau_{1/2} \approx 20$ min in C_6D_6 and 2–3 min in C_6D_5Br at room temperature.

The X-ray structure analysis of **4c**·0.5 Et_2O (Figure 2)[16] shows a trigonal-planar $B(C_6F_5)_2$ unit; one *o*-F atom is coordinated to the metal center ($\delta(^{19}F) = -179.8$). The ZrC_4 core has the familiar metallacyclopentene envelope conformation.

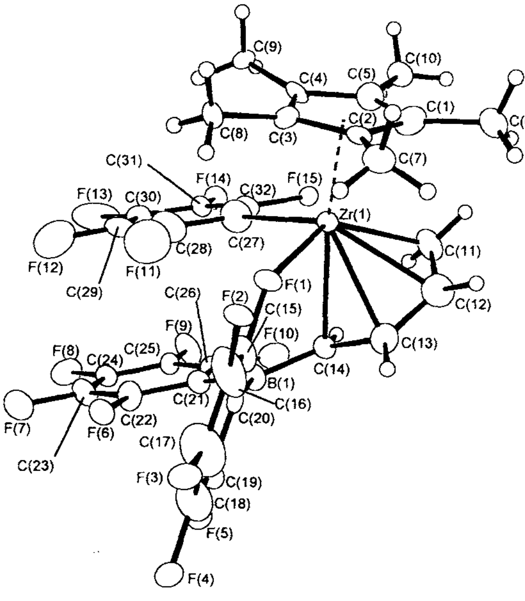

Figure 2. Structure of **4c**. Selected bond lengths [Å] and angles [°]: Zr(1)–C(11) 2.314(3), Zr(1)–C(12) 2.451(3), Zr(1)–C(13) 2.458(3), Zr(1)–C(14) 2.481(2), Zr(1)–C(27) 2.315(2), Zr(1)–F(1) 2.4292(15), C(11)–C(12) 1.414(4), C(12)–C(13) 1.375(4), C(13)–C(14) 1.454(3), B(1)–C(14) 1.488(3), B(1)–C(20) 1.582(4), B(1)–C(21) 1.590(3), C(15)–F(1) 1.380(3), C(19)–F(5) 1.351(3); F(1)-Zr(1)-C(27) 100.47(7), B(1)-C(14)-C(13) 126.3(2), C(11)-C(12)-C(13) 121.8(2), C(12)-C(13)-C(14) 120.5(2).

Surprisingly, the diene unit is oriented approximately orthogonal to the Cp ring and does not fall into either of the usual "prone" and "supine" categories.[17] The distribution of the bond lengths in the ZrC_4B unit, in particular the relatively short B–C(H) bond (1.485 Å), suggests that the zwitterionic resonance structure **B** may dominate over formulation **A**.[18]

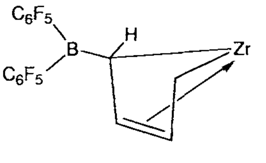

A

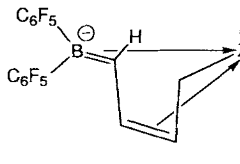

B

The results establish cationic 14-electron mono-Cp complexes as a new class of polymerization catalysts; their reactivity patterns, however, differ markedly from the behavior of the better-known di-Cp systems.

Experimental Section

All synthetic procedures were carried out under dry nitrogen using Schlenk techniques. NMR spectra were recorded on Bruker 300 and 500 MHz instruments. Compounds **1a**–**1c** were synthesized according to literature procedures [19].

2a: $B(C_6F_5)_3$ (0.89 g, 1.73 mmol) in toluene (20 mL) was added to a solution of **1a** (0.73 g, 1.72 mmol) in toluene (30 mL) at −78 °C. The mixture was stirred at this temperature for 30 min and then allowed to warm to room temperature. The color of the mixture changed instantaneously from red to dark orange. Concentration of the solution to 20 mL followed by cooling to −16 °C afforded orange crystals of **2a**·toluene (1.29 g, 1.38 mmol, 80%). Elemental analysis (%): Calcd for $C_{38}H_{36}BF_{15}Si_2Zr \cdot C_7H_8$: C 52.6, H 4.3; found: C 51.8, H 4.5.

3a: *t*BuNC (0.21 mL, 1.86 mmol) was added to a solution of **2a** (0.96 g, 0.93 mmol) in toluene (10 mL) at 0 °C. The resulting yellow mixture was concentrated and cooled to −16 °C to give yellow crystals of **3a** (0.79 g, 0.77 mmol, 83%). Elemental analysis (%): Calcd for $C_{43}H_{45}BF_{15}NSi_2Zr$: C 50.4, H 4.5, N 1.4; found: C 50.6, H 4.7, N 1.3. IR (Nujol): $\tilde{\nu} = 2179\ \mathrm{cm}^{-1}$ (C≡N).

2b: This compound is thermally sensitive and was therefore generated in solution and characterized spectroscopically. *$B(C_6F_5)_3$ (52 mg, 0.1 mmol) in* $[D_8]$toluene (0.2 mL) was added to a solution of **1b** (42 mg, 0.1 mmol) in $[D_8]$toluene (0.3 mL) at −60 °C. The orange solution contained **2b**, together with some **4b** and **4b′**.

4b: The compound was generated in situ from **1b** and $B(C_6F_5)_3$ (1 equiv) in $[D_8]$toluene at 0 °C; it slowly decomposed in solution at room temperature.

4c: A solution of $B(C_6F_5)_3$ (0.228 g, 0.44 mmol) in benzene (5 mL) was added to a solution of **1c** (0.148 g, 0.44 mmol) in benzene (5 mL) at room temperature. The resulting orange solution was stirred at ambient temperature for 40 min during which the solution turned red. The solvent was removed in vacuo and the residue was extracted with diethyl ether. Concentration and cooling of the solution to −70 °C yielded **4c**·0.5 Et_2O as a red crystalline solid (0.141 g, 0.20 mmol, 46%). Elemental analysis (%): Calcd for $C_{32}H_{20}BF_{15}Zr \cdot 0.5(C_2H_5)_2O$: C 48.8, H 3.0, Zr 10.9; found: C 48.5, H 3.0, Zr 10.8.

Received: April 14, 1997 [Z 10339 IE]
German version: *Angew. Chem.* **1997**, *109*, 2457–2460

Keywords: allyl complexes · C–H activation · diene complexes · homogeneous catalysis · zirconium

---

[1] M. Bochmann, *J. Chem. Soc. Dalton Trans.* **1996**, 255; H. H. Brintzinger, D. Fischer, R. Mülhaupt, B. Rieger, R. Waymouth, *Angew. Chem.* **1995**, *107*, 1255; *Angew. Chem. Int. Ed. Engl.* **1995**, *34*, 1143; M. Aulbach, F. Küber, *Chem. Unserer Zeit* **1994**, *28*, 197.

[2] A. M. Thayer, *Chem. Eng. News*, **1995**, Sept. 11, 15; *Chem. Br.* **1995**, 936; H. G. Hauthal, *Nachr. Chem. Tech. Lab.* **1995**, *43*, 822.

[3] G. G. Hlatky, H. W. Turner, R. R. Eckman, *J. Am. Chem. Soc.* **1989**, *111*, 2728.

[4] X. Yang, C. L. Stern, T. J. Marks, *J. Am. Chem. Soc.* **1991**, *113*, 3623; *ibid.* **1994**, *116*, 10015; M. Bochmann, S. J. Lancaster, M. B. Hursthouse, K. M. A. Malik, *Organometallics* **1994**, *13*, 2235.

[5] D. J. Gillis, M. J. Tudoret, M. C. Baird, *J. Am. Chem. Soc.* **1993**, *115*, 2543.

[6] M. Bochmann, G. Karger, A. J. Jaggar, *J. Chem. Soc. Chem. Commun.* **1990**, 1038.

[7] C. Pellecchia, A. Grassi, A. Immirzi, *J. Am. Chem. Soc.* **1993**, *115*, 1160; C. Pellecchia, A. Grassi, A. Zambelli, *J. Mol. Catal.* **1993**, *82*, 57.

[8] a) B. Temme, G. Erker, J. Karl, H. Luftmann, R. Fröhlich, S. Kotila, *Angew. Chem.* **1995**, *107*, 1867; *Angew. Chem. Int. Ed. Engl.* **1995**, *34*, 1755; b) B. Temme, J. Karl, G. Erker, *Chem. Eur. J.* **1996**, *2*, 919. For further examples for fluoroarylborate coordination see: X. Yang, C. L. Stern, T. J. Marks, *Organometallics* **1991**, *10*, 840; A. D. Horton, A. G. Orpen, *ibid.* **1991**, *10*, 3910; A. R. Siedle, R. A. Newmark, W. M. Lamanna, J. C. Huffman, *ibid.* **1993**, *12*, 1491; L. Lia, X. Yang, C. L. Stern, T. J. Marks, *ibid.* **1997**, *16*, 842.

[9] The coordinated *ortho*-F in $[Cp_2Zr\{C_3H_4CH_2B(C_6F_5)_3\}]$ experiences an upfield shift of about 80 ppm to $\delta = -213.2$ [8a].

[10] X-ray structure analysis of **2a**·toluene: An orange prism with dimensions 0.65 × 0.42 × 0.25 mm was grown from toluene and coated in perfluoropolyether RS3000 oil (Riedel De-Haën). $C_{38}H_{36}BF_{15}Si_2Zr \cdot C_7H_8$, $M_r = 1028.01$ (includes toluene molecule), triclinic, space group $P\bar{1}$, $a = 10.4955(12)$, $b = 13.538(2)$, $c = 16.650(2)$ Å, $\alpha = 77.695(11)$, $\beta = 83.542(10)$, $\gamma = 78.945(14)$°, $Z = 2$, $V = 2262.2(5)\ \text{Å}^3$, $\rho_{\text{calcd}} = 1.509\ \mathrm{Mg\,m^{-3}}$, $\mu = 3.344\ \mathrm{mm^{-1}}$, $F(000) = 1044$. Data collection was carried out at 160 K on a Stoe STADI4 four-circle diffractometer operating in the ω-θ scan mode using graphite-monochromated $Cu_{K\alpha}$ radiation ($\lambda = 1.54184$ Å). 7130 unique reflections were measured in the range $2.72 \leq \theta \leq 64.54°$ ($-12 \leq h \leq 12$, $-15 \leq k \leq 15$, $0 \leq l \leq 18$). The structure was solved by heavy atom methods using SHELXS-86 [20] and refined by full-matrix least-squares (against all the unique F^2 data) using SHELXL-93 [21]. Non-hydrogen atoms (including those of the toluene solvate molecule) were refined with anisotropic displacement parameters; hydrogen atoms were constrained to idealized positions by using a riding model with free rotation for methyl groups and fixed isotropic displacement parameters. Final $wR_2 = \{\sum[w(F_o^2 - F_c^2)^2]/\sum(F_o^2)^2]\}^{-1} = 0.1542$, conventional $R = 0.0530$ for F values of 6699 reflections with $F_o^2 > 2\sigma(F_o^2)$. Weighting scheme $w = [\sigma^2(F_o^2) + (0.0584\,P)^2 + 12.2995\,P]^{-1}$, where $P = (F_o^2 + 2F_c^2)/3$, goodness of fit = 1.069 for all F^2 values and 618 parameters. Maximum and minimum residual electron density 1.13 and −1.15 $e\text{Å}^3$, respectively [16b].

[11] Similar agostic interactions of two of the three methyl hydrogen atoms are found *in* $[(1,2\text{-}C_5H_3Me_2)_2ZrMe(\mu\text{-}Me)B(C_6F_5)_3]$ [Zr···H = 2.25(3) and 2.30(3) Å], while $[Cp_2ZrMe(\mu\text{-}Me)B(C_6F_5)_3]$ shows rather weaker agostic interactions [Zr···H 2.44(3) and 2.47(3) Å] [4].

[12] C. R. Patrick, G. S. Prosser, *Nature* **1966**, *187*, 1021; J. H. Williams, J. K. Cockcroft, A. N. Fitch, *Angew. Chem.* **1992**, *104*, 1666; *Angew. Chem. Int. Ed. Engl.* **1992**, *31*, 1655; J. H. Williams, *Acc. Chem. Res.* **1993**, *26*, 593.

[13] The "constraint geometry" complexes $[(C_5Me_4SiMe_2N\textit{t}Bu)Ti(C_4H_4R_2)]$ in the presence of $B(C_6F_5)_3$ are highly active for the copolymerization of ethene with 1-octene: D. D. Devore, F. J. Timmers, D. L. Hasha, R. K. Rosen, T. J. Marks, P. A. Deck, C. L. Stern, *Organometallics* **1995**, *14*, 3132. The living ethene oligomerization with activator-free $[(C_5Me_5)ZrR(2,3\text{-}Me_2C_4H_4)]$ has recently been reported: B. Hessen and H. van der Heijden, *J. Am. Chem. Soc.* **1996**, *118*, 11670.

[14] By contrast, propene polymerizations with $[Cp^*TiMe_3]/B(C_6F_8)_3$ give polymers with very narrow polydispersities and living characteristics: J. Sassmannshausen, M. Bochmann, J. Rösch, D. Lilge, *J. Organomet. Chem.*, in press.

[15] In contrast to the facile transfer of a C_6F_5 substituent from $B(C_6F_5)_3$ to a Zr atom, $B(C_6F_5)_3$ is inert towards electrophiles such as BBr_3 or Br_2. C_6F_5 transfer has been observed before at higher temperature and prolonged reaction times: R. Gomez, M. L. H. Green, J. L. Haggit, *J. Chem. Soc. Dalton Trans.* **1996**, 939.

[16] a) X-ray structure analysis of **4c**·0.5 Et_2O: an orange-red parallelepiped with dimensions 0.15 × 0.17 × 0.50 mm was grown from diethyl ether. Data were collected at 130 K. $C_{32}H_{20}BF_{15}Zr \cdot 0.5(C_2H_5)_2O$, $M_r = 828.58$, monoclinic $P2_1/n$, $a = 12.903(1)$, $b = 18.430(1)$, $c = 13.389(1)$ Å, $\beta = 96.08(1)°$, $V = 3166.0(4)\ \text{Å}^3$, $Z = 4$, $\rho_{\text{calcd}} = 1.738\ \mathrm{Mg\,m^{-3}}$, $\mu = 4.64\ \mathrm{cm^{-1}}$, 5128 reflections with $F_o \geq 4.0\sigma(F_o)$, 566 refined parameters. Data collection was carried out on an Enraf-Nonius CAD-4F^2 diffractometer using graphite-monochromated $Mo_{K\alpha}$ radiation ($\lambda = 0.71073$ Å; $\Delta\omega = 0.90 + 0.34\tan\theta$). 6264 Unique reflections were measured in the range $2.2 \leq 2\theta \leq 56.0°$ ($-15 \leq h \leq 8$, $-1 \leq k \leq 20$, $0 \leq l \leq 17$). The structure was solved by Patterson methods and extension of the model was accomplished by direct methods applied to differene structure factors using the program DIRDIF [23]. The structure was refined by full-matrix least-squares (SHELXL93 [21]). Non-hydrogen atoms were refined with anisotropic displacement parameters. The diethyl ether solvent molecule was highly disordered over an inversion center. The programs PLATON [24] (calculation of geometric data) and PLUTO [25] (structure diagram) were used. Final $wR_2 = \{\sum[w(F_o^2 - F_c^2)^2]/\sum(F_o^2)^2]\}^{-1} = 0.0783$, conventional $R = 0.0318$ for F values of 5128 reflections with $F_o^2 > 2\sigma(F_o^2)$. Weighting scheme $w = [\sigma^2(F_o^2) + (0.0429\,P)^2 + 1.6097P]^{-1}$, where $P = (F_o^2 + 2F_c^2)/3$, goodness of fit = 1.066 for all F^2 values and 566 parameters. Maximum and minimum residual electron density 0.54 and −0.48 $e\text{Å}^3$, respectively. b) Crystallographic data (excluding structure factors) for the structures reported in this paper have been deposited with the Cambridge Crystallographic Data Centre as supplementary publication no. CCDC-100329. Copies of the data can be obtained free of charge on application to The Director, CCDC, 12 Union Road, Cambridge CB2 1EZ, UK (fax: Int. code +(1223) 336-033; e-mail: deposit@chemcrys.cam.ac.uk).

[17] H. Yamamoto, H. Yasuda, K. Tatsumi, K. Lee, A. Nakamura, J. Chen, Y. Kai, N. Kasai, *Organometallics* **1989**, *8*, 105.

[18] For a discussion of B–C bond lengths see: G. Herberich, A. Fischer, *Organometallics* **1996**, *15*, 58, and references therein.

[19] J. B. Blenkers, H. J. de Liefde Meijer, J. H. Teuben, *J. Organomet. Chem.* **1981**, *218*, 383; G. Erker, K. Berg, R. Benn, G. Schroth, *Chem. Ber.* **1985**, *118*, 1383; J. Blenkers, B. Hessen, F. van Bolhuis, A. J. Wagner, J. H. Teuben, *Organometallics*, **1987**, *6*, 459.

[20] G. M. Sheldrick, *Acta Crystallogr. Sect. A*, **1990**, *46*, 467.

[21] G. M. Sheldrick, SHELXL-93, Program for refinement of crystal structures, Universität Göttingen, **1993**.

[22] P. McArdle, *J. Appl. Crystallogr.* **1995**, *28*, 65.

[23] P. T. Beurskens, G. Beurskens, W. P. Bosman, R. de Gelder, S. Gracía-Granda, R. O. Gould, R. Israel, J. M. M. Smits, the DIRDIF-96 program system, University of Nijmegen, **1996**.

[24] A. L. Spek, PLATON, program for automated analysis of molecular geometry, University of Utrecht, **1996**.

[25] A. Meetsma, PLUTO, program for the display and analysis of crystal and molecular structures, University of Groningen, **1996**.

0570-0833/97/3621-2361 $ 17.50+.50/0